Procedure of Equilibrium Measurements. Number of Ligand Molecules Participating in Complexation with Macrocyclic Ligand 1 or Monomeric Ligand 2. Aqueous uranyl tricarbonate (0.2 mM) was mixed with aqueous **1**·3Na (0.6–6.4 mM) with a carbonate buffer at pH 9.5. The absorbance of UO_2·**1**$^-$ at 450 nm was measured with a Union SM 401 spectrophotometer. Aqueous uranyl nitrate (2.0 mM) was mixed with aqueous sodium diethyldithiocarbamate (2.0–10.0 mM) for the measurement of the UO_2·**2** formation equilibrium.

Equilibrium Measurements. A quantity of 0.1 mM aqueous uranyl tricarbonate was mixed with aqueous sodium diethyldithiocarbamate in 20 mM carbonate buffer, pH 9.05. The initial concentration of sodium diethyldithiocarbamate ranged from 25 to 800 mM. The absorbance change at 450 and 480 nm was measured with a Union SM 401 spectrophotometer. Molar orders with respect to **2** for the first and third equilibrium steps are independently ascertained, as shown in Table I.

Estimation of Equilibrium Constants. Estimation of equilibrium constants were carried out on an NEC PC-8801 personal computer. In the course of the ligand-exchange reaction of $UO_2(CO_3)_3^{4-}$ with **2**, four different coordination states, $UO_2(CO_3)_3^{4-}$, $UO_2(CO_3)_2$·$\mathbf{2}^{3-}$, $UO_2(CO_3)$·$\mathbf{2}_2^{2-}$, and UO_2·$\mathbf{2}_3^-$, should be present as shown in eq 10. Under the present experimental conditions, the absorbance is expressed by eq 15 where the following assumptions are made:[19] $\epsilon_1 = \epsilon_0$, $\epsilon_2 = 2\epsilon_0$, $\epsilon_3 = 3\epsilon_0$.

$$\text{abs} = \epsilon_1[UO_2(CO_3)_2\cdot\mathbf{2}^{3-}] + \epsilon_2[UO_2(CO_3)\cdot\mathbf{2}_2^{2-}] + \epsilon_3[UO_2\cdot\mathbf{2}_3^-]$$

$$K_1 = \frac{[UO_2(CO_3)_2\cdot\mathbf{2}^{3-}][CO_3^{2-}]}{[UO_2(CO_3)_3^{4-}][\mathbf{2}^-]}$$

$$K_2 = \frac{[UO_2(CO_3)\cdot\mathbf{2}_2^{2-}][CO_3^{2-}]^2}{[UO_2(CO_3)_2\cdot\mathbf{2}^{3-}][\mathbf{2}^-]^2} \qquad K_3 = \frac{[UO_2\cdot\mathbf{2}_3^-][CO_3^{2-}]^3}{[UO_2\cdot(CO_3)\mathbf{2}_2^{2-}][\mathbf{2}^-]^3} \tag{15}$$

The absorbance is also expressed by eq 16 by using the equilibrium relationship. The initial (before iterating) values of K_1 and K_3 were

$$\text{abs} = \frac{[UO_2^{2+}]_T\epsilon_0 K_1\dfrac{[\mathbf{2}^-]}{[CO_3^{2-}]}}{1 + K_1\dfrac{[\mathbf{2}^-]}{[CO_3^{2-}]} + K_1K_2\dfrac{[\mathbf{2}^-]^2}{[CO_3^{2-}]^2} + K_1K_2K_3\dfrac{[\mathbf{2}^-]^3}{[CO_3^{2-}]^3}} \times \left(1 + 2K_2\frac{[\mathbf{2}^-]}{[CO_3^{2-}]} + 3K_2K_3\frac{[\mathbf{2}^-]^2}{[CO_3^{2-}]^2}\right) \tag{16}$$

obtained from the titration curve. Initial values of K_2 were obtained so as to give a best fit to the titration curve. Then, the iteration continued until the values of K_1, K_2, and K_3 giving the "best fit" titration curve were obtained.

Registry No. **1**, 89438-89-1; **2**, 147-84-2; $UO_2(CO_3)_3^{4-}$, 24646-13-7.

(19) As shown in Figure 3, the "total" absorbance of uranyl diethyldithiocarbamate complex increased in proportion to $[\mathbf{2}^-]$ till the $[\mathbf{2}^-]/[UO_2^{2+}]$ ratio reached the established stoichiometry[12] of 3. The observation clearly indicates not only that equilibrium proceeds successively U → **2**·U → $\mathbf{2}_2$U → $\mathbf{2}_3$U (see text) but also that all the absorption coefficients of the dithiocarbamate chromophore of **2**·UO_2, $\mathbf{2}_2UO_2$, and $\mathbf{2}_3UO_2$ at 450 nm are equal. In other words, the assumption that ϵ_2 equaled $2\epsilon_1$ and ϵ_3 equaled $3\epsilon_1$ must be satisfied.

Contribution from the Chemical Research Institute of Non-aqueous Solutions, Tohoku University, Katahira, Sendai, Japan 980

Correlation between the Hyperfine Coupling Constants of Donor Nitrogens and the Structures of the First Coordination Sphere in Copper Complexes As Studied by ^{14}N ENDOR Spectroscopy

Masamoto Iwaizumi,* Takanori Kudo, and Shouichi Kita[1]

Received April 8, 1985

Hyperfine (hf) coupling constants of coordinating nitrogens in copper(II) complexes with a pseudoplanar coordination array were collected with the help of ^{14}N ENDOR spectroscopy. The hf coupling constants are well grouped by the donor sets, N_4, *cis*-N_2O_2, *trans*-N_2O_2, and NO_3, as well as by the hybridized state of the nitrogens. Ligation at the axial position or distortion of the coordination array from planar to tetrahedral leads to decrease of the hf coupling constants. These correlations with the coordination structures indicate that the hf coupling constants of donor atoms may be useful to infer donor atoms and their configuration in the first coordination sphere for complexes with unknown metal binding sites, in conjunction with ESR or other studies.

Electron–nuclear double resonance (ENDOR) has been successfully used for resolving ligand hyperfine (hf) couplings buried in the ESR line widths in metal complexes.[2] In some cases, ligand hf interactions have been useful for obtaining information of structural details or for estimation or confirmation of metal binding sites. In the present work, we collected hf coupling constants of donor nitrogens in copper(II) complexes by the use of ENDOR spectroscopy, with the aim of finding general trends of the hf coupling constants of donor nitrogens and to find any correlation with the coordination structure. The copper(II) complexes treated here are limited to those having basically pseudoplanar array and donor sets of N_4, *cis*-N_2O_2, *trans*-N_2O_2, and NO_3. Frozen solutions and powder samples of the copper complexes were used for the ENDOR measurements in this work. The collected ^{14}N hf coupling data are well related to the donor sets and the hybrid state of nitrogens.

Experimental Section

Copper(II) complexes treated in this paper are listed in Table I. These complexes were synthesized according to literature cited in the table except for a few cases where a minor modification was made. Synthesized complexes were identified by elemental analyses and, for some cases, by also using optical absorption spectroscopy. Measurements of ENDOR spectra were made by a Varian E1700 ENDOR spectrometer at 10–25 K. The temperatures were controlled by a helium gas flow type cryostat.

Results and Discussion

The ESR spectrum of [Cu(aema)] and its ENDOR spectra recorded by different magnetic field settings indicated in the ESR spectrum are shown in Figures 1 and 2 as an example. In Figure 2, ^{14}N ENDOR signals due to two nonequivalent nitrogens are observed. As will be discussed later, the nitrogen signals on the low-frequency side can be assigned to the amine nitrogens and

(1) Present address: Department of Chemistry, Faculty of Science, Hirosaki University, Bunkyo-cho, Hirosaki, Japan 036.
(2) Schweiger, A. *Struct. Bonding (Berlin)* **1982**, *51*, 1.

0020-1669/86/1325-1546$01.50/0 © 1986 American Chemical Society

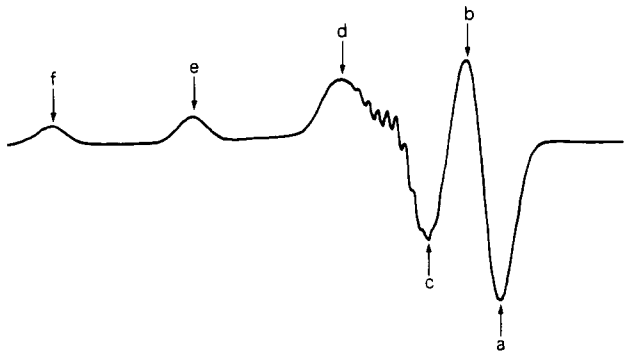

Figure 1. ESR spectrum of a frozen H_2O–MeOH (1:1) solution of [Cu(aema)]. The sample was 3 mM in the complex. Instrumental conditions: temperature, 70 K; microwave power, 5mW; microwave frequency, 9.315 GHz, field modulation, 3 G_{p-p} at 100 kHz; sweep, 1 kG in 8 min; time constant, 0.25 s. The arrows mark the positions where the ENDOR spectra in Figure 2 were recorded. ^{1}H resonance frequencies at the arrow positions: (a) 14.447 MHz; (b) 14.229 MHz; (c) 13.999 MHz; (d) 13.451 MHz; (e) 12.523 MHz; (f) 11.649 MHz.

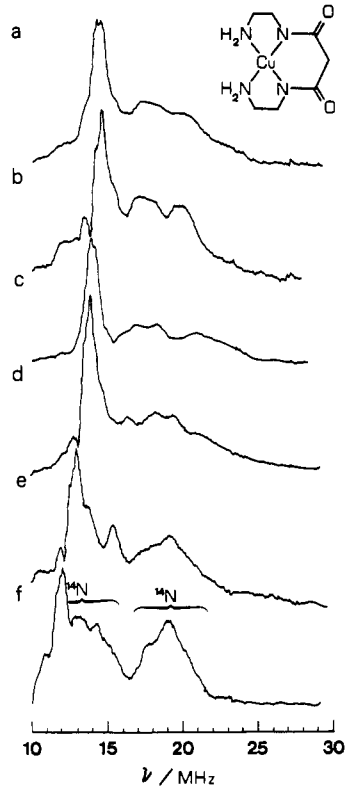

Figure 2. ENDOR spectra of a frozen H_2O–MeOH (1:1) solution of [Cu(aema)]. The sample is the same as in Figure 1. Spectra a–f were recorded by setting the magnetic field at the arrow positions a–f in Figure 1, respectively. Instrumental conditions: temperature, 17–20 K; microwave power, 3.5 mW; microwave frequency, 9.318 GHz; field modulation, 6 G_{p-p} at 34.7 Hz; sweep rate, 20 MHz/16 min. Rf was amplified by the rf high power amplifier in a Varian E1700 instrument with amplitude modulation at 1 kHz and at 10% duty cycle, no accumulation.

those on the high-frequency side to the deprotonated amide nitrogens. The ENDOR spectra observed from frozen solutions or powder samples by setting an arbitrary point of the ESR spectra are superposition of the signals arising from the molecules, which orient to the external magnetic field so the following ESR resonance condition is satisfied.

$$h\nu_{ESR} = g\beta H + K^{Cu}M_I^{Cu} + \frac{1}{4g\beta H}\{[I^{Cu}(I^{Cu}+1) - (M_I^{Cu})^2]\ \mathrm{Tr}\ \tilde{\mathbf{A}}^{Cu}\cdot\mathbf{A}^{Cu} - 2(M_I^{Cu})^2(K^{Cu})^2 - [I^{Cu}(I^{Cu}+1) - 3(M_I^{Cu})^2]\tilde{\mathbf{h}}\cdot\tilde{\mathbf{g}}\cdot\tilde{\mathbf{A}}^{Cu}\cdot\mathbf{A}^{Cu}\cdot\tilde{\mathbf{A}}^{Cu}\cdot\mathbf{A}^{Cu}\cdot\mathbf{g}\cdot\mathbf{h}/g^2(K^{Cu})^2\} + \sum K^{N_i}M_I^{N_i}$$

where

$$g = (\tilde{\mathbf{h}}\cdot\tilde{\mathbf{g}}\cdot\mathbf{g}\cdot\mathbf{h})^{1/2}$$

$$K^{Cu} = (\tilde{\mathbf{h}}\cdot\tilde{\mathbf{g}}\cdot\tilde{\mathbf{A}}^{Cu}\cdot\mathbf{A}^{Cu}\cdot\mathbf{g}\cdot\mathbf{h})^{1/2}/g$$

$$K^{Ni} = (\tilde{\mathbf{h}}\cdot\tilde{\mathbf{g}}\cdot\tilde{\mathbf{A}}^{N_i}\cdot\mathbf{A}^{N_i}\cdot\mathbf{g}\cdot\mathbf{h})^{1/2}/g$$

$$\mathbf{h} = \{\sin\theta\cos\phi,\ \sin\theta\sin\phi,\ \cos\theta\}$$

and where H is the external field strength at ENDOR measurements. Here, θ and ϕ are the polar and azimuthal angles in the g tensor frame.

When the magnetic field is fixed at the g extreme of the ESR spectra (Figure 1, point f), ENDOR spectra become a single crystallike pattern because the ENDOR signals come from only the molecules orienting so that their $g_\parallel$ direction is parallel to the external field ($\theta = 0$).[3-5] In such a case, the ^{14}N ENDOR spectra show a characteristic pattern given, in the first order, by $\nu^N = |A^N/2 \pm \nu_N \pm q^N|$, where A^N is the hf coupling in the $g_\parallel'$ direction, ν_N the Zeeman splitting, and Q^N the quadrupole coupling. Though there are cases where the Zeeman or quadrupole couplings cannot be well resolved, the $A^N/2$ value can be easily determined from the center of the ^{14}N signals as far as the whole ^{14}N ENDOR pattern can be observed. As the field set position moves from the $g_\parallel$ extreme toward the $g_\perp$ region, θ and ϕ diverge, though they are still in some limited range, and the single-crystal-like nature in the ENDOR spectra is lost. Examination of the angle-selected spectra obtained by changing the external field set positon will make possible to obtain hf tensor components and their relative orientation to the g tensor axes. However, when the hf and quadrupole interactions have large anisotropies, the powder ENDOR signals diverges to a relatively wide frequency range, and to obtain reliable anisotropic hf and quadrupole coupling values, observation of ENDOR spectra having well-defined line shapes becomes essential. In the present case, however, there were many cases where the observation of such spectra was difficult, and in some cases overlap of ^{1}H ENDOR with ^{14}N ENDOR made the analysis more difficult. Though the anisotropic nature of the hf interactions may provide more structural details,[2,6-9] we limit, therefore, discussion to the magnitudes of hf couplings in the $g_\parallel$ direction which are obtainable most easily for most copper complexes.

As is shown in Figure 2, ^{14}N ENDOR signals are sometimes located close to the free proton frequency and overlap with ^{1}H signals. In such cases, use of D_2O, methanol-d_4, or methanol-D as solvents was effective to distinguish the ^{14}N ENDOR signals by removing matrix ENDOR and ligand exchangeable ^{1}H signals. Different temperature and concentration dependencies between the ^{1}H and ^{14}N signal intensities were sometimes useful to distinguish ^{14}N signals from ^{1}H signals. However, in several cases, a reliable determination of the ^{14}N coupling constants was still difficult due to the overlap with ^{1}H ENDOR signals.

^{14}N ENDOR signals observed in the present experiments in the 10–25-MHz range can be attributed to the nitrogens in the first coordination sphere of the pseudo-planar array; ENDOR signals arising from the nitrogens at the axial position or other ligand nitrogens are expected to be observed at the lower frequency region. The obtained coupling constants are listed in Table I,

(3) Rist, G. H.; Hyde, J. S. *J. Chem. Phys.* **1970**, *52*, 4633.
(4) Hoffman, B. M.; Martinsen, J.; Venters, R. A. *J. Magn. Reson.* **1984**, *59*, 110.
(5) Hoffman, B. M.; Venters, R. A.; Martinsen, J. *J. Magn. Reson.* **1985**, *62*, 537.
(6) Yokoi, H.; Ohba, Y.; Takabe, T. *Biochem. J.* **1983**, *215*, 209.
(7) Van Camp, H. L.; Sands, R. H.; Fee, J. A. *J. Chem. Phys.* **1981**, *75*, 2098.
(8) Yokoi, H. *Biochim. Biophys. Res. Commun.* **1982**, *108*, 1278.
(9) Roberts, J. E.; Cline, J. F.; Lum, V.; Freeman, H.; Gray, H. B.; Peisach, J.; Reinhammar, B.; Hoffman, B. M. *J. Am. Chem. Soc.* **1984**, *106*, 5324.
(10) Tschugaeff, L. *Z. Anorg. Chem.* **1905**, *46*, 144.
(11) Tomoda, H.; Saito, S.; Shirai, S. *Chem. Lett.* **1983**, 313.
(12) Kedzia, B. B.; Armendarez, P. X.; Nakamoto, K. *J. Inorg. Nucl. Chem.* **1968**, *30*, 849.
(13) (a) Malatesta, V.; McGarvey, B. R. *Can. J. Chem.* **1975**, *53*, 3791. (b) Green, M.; Tasker, P. A. *J. Chem. Soc. A* **1970**, 2531, 3105.

Table I. ^{14}N Hyperfine Coupling Constants in the $g_{\parallel}$ Direction Obtained by ENDOR

no.	complex[a]	medium[b]	A^N/MHz	ref c	ref d	no.	complex[a]	medium[b]	A^N/MHz	ref c	ref d
1	$[Cu(dmg)_2]$	$[Ni(dmg)_2]$	47.2		33	38	[Cu(salap)]	toluene–py	35.4	22	
2		toluene–py	45.8	10		39	$[Cu(sal)_2]$	$[Ni(sal)_2]$	33.5	23	
3	[Cu(pc)]	[Ni(pc)]	46.8	11		40	$[Cu(esal)_2]$	toluene	33.3	23	
4		[Zn(pc)]	46.3			41	$[Cu(npsal)_2]$	toluene	32.4	23	
5		H_2pc	45.9			42	$[Cu(ipsal)_2]$	toluene	32.3	23	
6	$[Cu(biu)_2]^{2-}$	8 N KOH_{aq}–MeOH	44.9	12		43	$[Cu(nbsal)_2]$	toluene	32.3	23	
7	[Cu(oep)]	toluene–TNB	44.3		34	44	$[Cu(pymth)_2]$	H_2O–diol	32.3	24	
8		toluene	43.8		34	45	$[Cu(ibsal)_2]$	toluene	32.2	23	
9		toluene–py	41.5		34	46	$[Cu(chsal)_2]$	toluene	32.0	23	
10	[Cu(tpp)]	$[Zn(tpp)]\cdot H_2O$	44.965		35	47	$[Cu(sbsal)_2]$	toluene	29.8	23	
11		toluene–TNB	43.9		34	48	$[Cu(meqn)_2]$	$[Zn(meqn)_2]\cdot xH_2O$	29.0		35
12		toluene	43.6		34	49	$[Cu(qn)_2]$	Hqn	27.5	25	
13		toluene–py	41.1		34	50		phthalimide	30.3		35
14	[Cu(amben)]	[Ni(amben)]	43.1	13		51	$[Cu(tbsal)_2]$	toluene	29	23	
15	$[Cu(im^-)_2]$	$[Zn(im^-)_2]$	41.6		6	52	$[Cu(salox)_2]$	$[Pd(salox)_2]$	43.8		35
16	$[Cu(im)_4]^{2+}$	pH 6.3–8.0, H_2O	40.3		6	53		$[Ni(salox)_2]$	43.64		32
17		pH 9.0, H_2O–triol	39.8		7	54		toluene–py	40.6	26	
18	$[Cu(im)_2(im^-)]NO_3$	$[Zn(im)_2(im^-)]NO_3$	39.6		6	55	$[Cu(NH_3)_4]^{2+}$	pH 10, H_2O	31.7		8
19	[Cu(aema)]	H_2O–MeOH	38.1	14		56	$[Cu(tn)_2]SO_4$	D_2O–MeOD	31.5	27	
			28.7			57	$[Cu(eten)_2](ClO_4)_2$	D_2O–MeOD	28	27	
20	$[Cu(im)_6]Cl_2\cdot 4H_2O$	$[Zn(im)_6]Cl_2\cdot 4H_2O$	33.4		6	58	$[Cu(pn)_2]SO_4$	D_2O–MeOD	28	27	
21	$[Cu(bslal)(H_2O)]$	H_2O–triol	41.7	15		59	$[Cu(en)_2]SO_4$	D_2O–MeOD	28	27	
22	$[Cu(slgl)(H_2O)]$	H_2O–triol	41.3	16		60		H_2O–triol	27		
23	$[Cu(slal)(H_2O)]$	H_2O–triol	41.0	15		61		pH 10 H_2O	28		
24	$[Cu(nslal)(H_2O)]$	H_2O–triol	41.0	15		62	$[Cu(meen)_2]SO_4$	H_2O–diol	27	27	
25	$[Cu(pyvbl)(H_2O)]$	H_2O–MeOH	40.5	17		63	[Cu(glglgl)]	pH 3.5, H_2O–triol	29	28	
26	$[Cu(pyval)(H_2O)]$	H_2O–EtOH	38.1	17		64	$H_2[Cu(pdta)]$	H_2O–triol	28	29	
27	[Cu(acen)]	toluene	39.1	18		65	$H_2[Cu(edta)]$	D_2O–MeOD	28	29	
28		toluene–py	37.7			66	$[Cu(en)(H_2O)_2]SO_4$	D_2O–MeOD	26	30	
29	[Cu(salen)]	[Ni(salen)]	39.1		36	67	$[Cu(gly)_2]$	pH 10, H_2O	29.3		8
			38.8			68		D_2O–MeOD	24	31	
30		toluene–py	37.2	19		69		Hgly	17.40		37
31	[Cu(salph)]	[Ni(salph)]	37.9	19		70	$[Cu(ala)_2]$	Hala	27.38		38
32	[Cu(facen)]	toluene–py	37.0	20		71		Hala	27.07		39
33	[Cu(saltn)]	EtOH	36.6	19		72	$[Cu(pro)_2]$	D_2O–MeOD	27	31	
34		toluene–py	36.2			73	$[Cu(ser)_2]$	D_2O–MeOD	24	31	
35	$[Cu(pic)_2]$	phthalic acid	36.9		35	74	$[Cu(val)_2]$	D_2O–MeOD	24	31	
36		toluene–py	34.5	21		75	$[Cu(\beta ala)_2]$	D_2O–MeOD	23.6	30	
37		$[Zn(pic)_2]\cdot 4H_2O$	29.7			76	$[Cu(thr)_2]$	D_2O–MeOD	23	30	

[a] Key: Hdmg, dimethylglyoxime; H_2pc, phthalocyanine; H_2biu, imidodicarbonic diamide; H_2oep, octaethylporphine; H_2tpp, tetraphenylporphine; H_2amben, *N,N'*-ethylenebis((*o*-aminobenzilidene)amine); Him, imidazole; H_2aema, *N,N'*-bis(2-aminoethyl)malonamide; H_2bslal, *N*-(5-bromosalicylidene)alanine; H_2slgl, *N*-salicylideneglycine; H_2slal, *N*-salicylidenealanine; H_2nslal, *N*-(5-nitrosalicylidene)alanine; H_2pyvgl, *N*-pyruvylideneglycine; H_2pyval, *N*-pyruvylidene-β-alanine; H_2acen, *N,N'*-ethylenebis(acetylacetone imine); H_2salen, *N,N'*-ethylenebis(salicylideneamine); H_2salph, *N,N'*-phenylenebis(salicylideneamine); H_2facen, *N,N'*-ethylenebis((trifluoroacetyl)acetone imine); H_2saltn, *N,N'*-trimethylenebis(salicylideneamine); Hpic, 2-pyridinecarboxylic acid; H_2salap, *N*-salicylidene-*o*-aminophenol; Hsal, *N*-salicylideneamine; Hesal, *N*-salycylideneethylamine; Hnpsal, *N*-salicylidene-*n*-propylamine; Hipsal, *N*-salicylideneisopropylamine, Hnbsal, *N*-salicylidene-*n*-butylamine; Hchsal, *N*-salicylidenecyclohexylamine; Hibsal, *N*-salicylideneisobutylamine; Hsbsal, *N*-salicylidene-*sec*-butylamine; Htbsal, *N*-salicylidene-*tert*-butylamine; Hpymth, 2-pyridylmethanol; Hmeqn, 2-methyl-8-quinolinol; Hqn: 8-quinolinol; Hsalox, salicylaldoxime; tn, trimethylenediamine; eten, *N,N*-diethylethylenediamine; pn, 1,2-propanediamine; en, ethylenediamine; glglgl, glycylglycylglycine; H_4pdta, propylenediaminetetraacetic acid; H_4edta, ethylenediaminetetraacetic acid, Hgly, glycine; Hala, L-alanine; Hβala, β-alanine; Hpro, L-proline; Hser, L-serine; Hval, valine; Hthr, L-threonine; meen, *N,N'*-dimethylethylenediamine. [b] Key: py, pyridine; MeoH, methanol; MeOD, methanol-*d*; EtOH, ethanol; diol, ethylene glycol; triol, glycerol. [c] References for complex preparation. [d] References for ENDOR data.

together with the data already reported in the literature.

Figure 3 shows plots of the hf coupling data, and it shows that the magnitude of ^{14}N hf coupling constants are grouped by the donor sets; i.e., they tend to decrease in the order N_4, NO_3, *cis*-N_2O_2, and *trans*-N_2O_2. They are also affected by hybridized states of the nitrogen orbitals; i.e., the nitrogens with planar conformation such as deprotonated amide nitrogens and aromatic aza nitrogens have larger coupling constants than those for nitrogens with tetrahedral conformations such as amine nitrogens.

(14) Ojima, H.; Yamada, K. *Nippon Kagaku Zasshi* **1970**, *91*, 49.
(15) Nakao, Y. *Nippon Kagaku Zasshi.* **1971**, *92*, 399.
(16) Nakahara, A. *Bull. Chem. Soc. Jpn.* **1959**, *32*, 1195.
(17) Nakahara, A.; Yamamoto, H.; Matsumoto, H. *Bull. Chem. Soc. Jpn.* **1964**, *37*, 1137.
(18) Ueno, K. *Chelate Kagaku*; Nankodo: Tokyo, 1975; p 449.
(19) Pfeiffer, P. J.; Breith, E.; Lubbe, E.; Tsumaki, T. *Justus Liebigs Ann. Chem.* **1933**, *503*, 84.
(20) McCarthy, P. J.; Hovey, R. J.; Ueno, K.; Martell, A. E. *J. Am. Chem. Soc.* **1955**, *77*, 5820.
(21) Cox, E. G.; Wardlaw, W.; Webster, K. C. *J. Chem. Soc.* **1936**, 775.
(22) Bereman, R. D.; Shilds, G. D.; Dorfman, J. R.; Bondner, J. *J. Inorg. Biochem.* **1983**, *19*, 75.
(23) Sacconi, L.; Smith, J. W. *J. Chem. Soc.* **1956**, 1821.
(24) Murakami, T.; Takui, M. *Bull. Chem. Soc. Jpn.* **1965**, *38*, 828.
(25) Bailey, A. S.; William, R. J. P.; Wright, J. D. *J. Chem. Soc.* **1965**, 2579.
(26) (a) Cox, E. G.; Webster, K. C. *J. Chem. Soc.* **1935**, 731. (b) Cox, E. G.; Pinkard, F. W.; Wardlaw, W.; Webster, K. C. *J. Chem. Soc.* **1935**, 759.
(27) Pfeiffer, P.; Glaster, H. *J. Prakt. Chem.* **1938**, *151*, 134.
(28) Crawford, T. H.; Dalton, J. O. *Arch. Biochem. Biophys.* **1969**, *131*, 123.
(29) Kishner, S. *J. Am. Chem. Soc.* **1956**, *78*, 2372.
(30) Grosson, H.; Schuck, B. *Z. Anorg. Chem.* **1906**, *50*, 1.
(31) Takui, T. *Bull. Chem. Soc. Jpn.* **1965**, *38*, 1726.
(32) Schweiger, A.; Gunthard, H. H. *Chem. Phys.* **1978**, *32*, 35.
(33) Rist, G. H.; Hyde, J. S. *J. Chem. Phys.* **1970**, *52*, 4633.
(34) Iwaizumi, M.; Ohba, Y.; Iida, H.; Hirayama, M. *Inorg. Chim. Acta* **1984**, *82*, 47.
(35) Brown, T. G.; Hoffman, B. M. *Mol. Phys.* **1980**, *39*, 1073.
(36) Kita, S.; Hashimoto, M.; Iwaizumi, M. *Inorg. Chem.* **1979**, *18*, 3432.
(37) Fujimoto, M.; McDowell, C. A.; Takui, T. *J. Chem. Phys.* **1979**, *70*, 3694.
(38) Calvo, R.; Oseroff, S.; Abache, H. C. *J. Chem. Phys.* **1980**, *72*, 760.
(39) McDowell, C. A.; Naito, A. *J. Magn. Reson.* **1981**, *45*, 205.

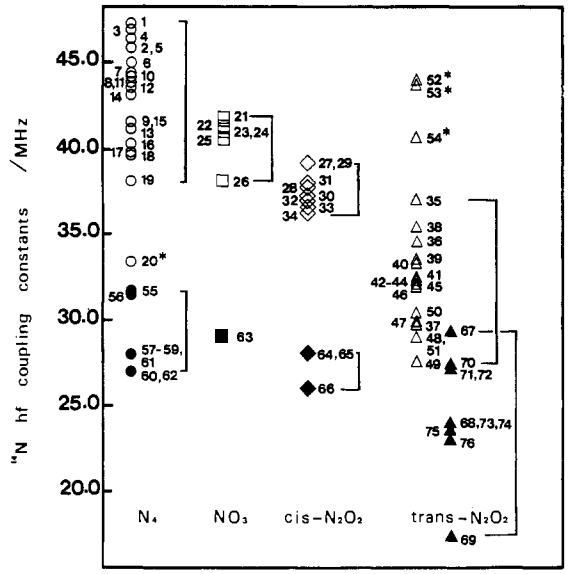

Figure 3. Plots of A^N values. Each number corresponds to the sample number in Table I. Open marks are for sp^2 type nitrogens, and solid marks are for sp^3 type. Sample numbers denoted by an asterisk are discussed in the text.

The ^{14}N hf couplings observed from solid samples such as frozen solutions or powders arise from the interactions with the unpaired spin on copper orbitals and that delocalized on the nitrogen orbitals. Assuming the unpaired electron densities on the copper to be 0.7–0.8 as evaluated for ordinary copper complexes by ESR analyses, the contribution of the unpaired electron on copper is calculated to be about 1–2 MHz. Therefore, the main part of the observed nitrogen hf coupling constants (47–20 MHz) can be regarded as arising from the unpaired electrons delocalized on the nitrogens.

Theoretical calculation predicts that an unpaired electron on the nitrogen 2p orbital gives an hf coupling constant of 47.8 MHz, while that on the nitrogen 2s orbital gives 1540 MHz,[40] which is much larger than the former, suggesting that the unpaired spin on the nitrogen orbitals having a higher s/p hybrid ratio will give a larger hf coupling constant. This is in good accord with the observed trends that the nitrogens having planar conformation, sp^2 type conformation, show larger hf coupling constants than the nitrogens having tetrahedral, sp^3, conformation.

If the hybridization of the coordinating orbitals of the nitrogens is known, approximate spin densities on the nitrogen orbitals can be estimated from the experimental hf coupling constants by using the theoretical values, 47.8 and 1540 MHz. Taking the coordinating orbitals of deprotonated amide and aromatic aza nitrogens to be pure sp^2 hybridized orbitals and those of amine nitrogens to be pure sp^3, respectively, the spin densities for the former case are calculated to be 0.086–0.068 (N_4), 0.077–0.070 (NO_3), 0.072–0.066 (*cis*-N_2O_2), and 0.068–0.050 (*trans*-N_2O_2) for each donor set and those for the latter case are calculated to be 0.075–0.066 (N_4), 0.069–0.066 (NO_3), 0.066–0.062 (*cis*-N_2O_2), and 0.070–0.045 (*trans*-N_2O_2). The spin densities on the nitrogen atoms tend to decrease in the order N_4, NO_3, *cis*-N_2O_2, and *trans*-N_2O_2. One can see also that the spin densities on the nitrogens in the sp^3 state are slightly less than those on the nitrogens in the sp^2 state.

The fact that the ^{14}N hf couplings or the spin densities on the nitrogens change with the donor sets in the pseudoplanar array may be attributed to changes in hybridization of the copper unpaired electron orbitals. It affects the overlap with the donor atom orbitals and hence the delocalization of the unpaired electron onto the ligands. In N_4 type complexes, the unpaired electron orbital of copper is $3d_{xy}$ under pseudo-D_{4h} symmetry, while in *cis*-N_2O_2 type complexes the $4p_x$ orbital mixes with the unpaired electron orbital, $3d_{xy}$, (the C_{2v} symmetry axis is y) under the pseudo-C_{2h} symmetry, and in *trans*-N_2O_2 having pseudo-D_{2h} symmetry, the 4s orbital mixes with the $3d_{xy}$ orbital. As the crystalline field of nitrogen is stronger than that of oxygen, the orbital mixing will occur so that the orbital spread toward the nitrogens is reduced and that toward the oxygens expanded, resulting in a decrease of ^{14}N hf couplings. Smaller ^{14}N coupling constants in *trans*-N_2O_2 than in *cis*-N_2O_2 indicate that the mixing of 4s in *trans*-N_2O_2 is larger than that of $4p_x$ in *cis*-N_2O_2. In the case of NO_3 type complexes, the $3d_{xy}$ unpaired electron orbital can mix with 4s and 4p under the pseudo-C_{2h} symmetry. However, the orbital mixing may be not so large, as the unpaired electron delocalization is largely affected.

Effects of distortion from the planar array to the tetrahedral array in the first coordination sphere can be seen in the data of a series of N-substituted salicylaldehyde Schiff base complexes and for [Cu(salen)] and [Cu(saltn)]. In the former series the nitrogen hf coupling constant decreases by substitution of the N–H proton with a bulky alkyl group; i.e., it decreases in the order N–H, N–ethyl, N–*n*-propyl, N–isopropyl, N–*n*-butyl, N–isobutyl, N–cyclohexyl, N–*sec*-butyl, and N–*tert*-butyl derivatives. In the case of [Cu(salen)] and [Cu(saltn)], the latter, having a larger distortion from the planar array, shows a smaller nitrogen hf coupling than the former. These results indicate that distortion from the planar conformation results in reduction of overlap of the copper unpaired electron orbital with the ligands and hence causes decreases in the nitrogen coupling constants.

Axial ligation of nitrogen bases causes decreases in hf coupling constants of nitrogens at the equatorial plane as is seen from the data for solutions containing pyridine. On the other hand, interactions of copper(II) complexes with electron-acceptor molecules causes an increase of the coupling constants of nitrogens in the square-planar array (see data points no. 7 and 11 in Table I).[33] In general, electron-donating interactions at the axial position cause the decrease in nitrogen hf couplings and vice versa for electron-accepting interactions. However, the effects are not necessarily so large as those arising from changes in hybridization of nitrogen orbitals and changes in the donor sets in the pseudoplanar array except for some special cases as shown in the following.

The ^{14}N coupling constants of $[Cu(im)_6]Cl_2 \cdot 4H_2O$[6] and $[Cu(salox)_2]$[32,35] are the exceptional cases, which do not fit the classification shown in Figure 3. In the former, the copper ion is coordinated by six imidazole nitrogens and is nearly in the octahedral crystalline field. Appreciable reduction of the nitrogen coupling may be attributed to the strong axial field or dynamic Jahn–Teller effects. $[Cu(salox)_2]$, meanwhile, shows a ^{14}N coupling constant larger than the ones of the other *cis*-N_2O_2 complexes. The presence of the hydroxy group at the coordinating nitrogen and its formation of a hydrogen bond with the coordinating oxygen would weaken the crystalline field of the nitrogen and strengthen that of the oxygen. These effects would lead to the tetragonal crysalline field rather than the C_{2v} symmetry field due to the *cis*-N_2O_2 donor set and hence would lead to the large nitrogen hf coupling constant corresponding to the ones of the N_4 type complexes.

The results mentioned above indicate that the hf coupling constants of nitrogens in the first coordination sphere correlate well with the donor sets in the equatorial plane as well as with the kind of nitrogens, deprotonated amide nitrogens, aromatic aza nitrogens, or amine nitrogens. The correlation between ESR parameters ($g_\parallel$ and $A_\parallel^{Cu}$) donor atoms at the copper binding sites has been shown by Peisach and Blumberg.[41] Their correlation has been useful for estimating structures for copper proteins. The present results indicate that ^{14}N hf coupling constants may be also useful for estimation or confirmation of the structure of the copper binding sites in conjunction with the ESR or other studies. It should be noticed that nitrogen hf coupling data make possible to distinguish the type of nitrogens, sp^2 and sp^3, and the cis and trans configuration in N_2O_2 type complexes, though the $g_\parallel$ and

(40) Wertz, J. E.; Bolton, J. R. *Electron Spin Resonance: Elementary Theory and Practical Applications*; McGraw-Hill: New York, 1972.

(41) Peisach, J.; Blumberg, W. E. *Arch. Biochem Biophys.* **1974**, *165*, 691.

$A_{\parallel}^{Cu}$ correlation could not distinguish them. Examples of the use of the correlation in Figure 3 are shown in the following.

Recently, ^{14}N ENDOR[42] and X-ray[43] analysis data of the bovine superoxide dismutase (BSD) have been reported. According to the X-ray data, the copper ion in native BSD is coordinated by four imidazole nitrogens in a pseudo-square-planar plane with tetrahedral distortion. The ENDOR experiment shows that the coordinating nitrogens have a coupling constant of 38.7 MHz in the native form, though the value has been reported as tentative because of anisotropy and possible inequivalence of the nitrogens. According to Figure 3, the hf coupling constant corresponds to the lowest limit of the range of the N_4 coordination classification for deprotonated amide or aromatic aza nitrogens. As distortion from planar to tetrahedral makes ^{14}N hf coupling constants smaller, this observation of the ^{14}N hf coupling constants of BSD is quite consistent with the X-ray data assigning the copper binding site to the N_4 donor set due to four imidazole nitrogens with tetrahedral distortion.

The next example is the copper binding site in galactose oxidase, which is one of the type II copper proteins. According to ESR and electron spin echo studies, the copper binding site was estimated to be a N_2O_2 structure and imidazole nitrogens were assigned to the two nitrogens.[22,44] These two imidazole nitrogens have been supposed to be in the trans configuration. Bereman et al. obtained the coupling constant of the two nitrogens in the $g_{\parallel}$ direction to be 14.5 G (46.2 MHz) from ESR spectra.[44a] According to the above discussion, the assignment of the hf interacting nuclei to the imidazole nitrogens seems reasonable, because the coupling constant is in the range for the aromatic aza nitrogens. However, the hf coupling constant is closer to the range for the *cis*-N_2O_2 configuration than for the *trans*-N_2O_2 configuration, though it is slightly higher than the values for the *cis*-N_2O_2 type complexes. Taking into account the fact that coupling constants obtained by ESR may be less accurate than those obtained by ENDOR, the deviation from the cis range does not seem so serious. Therefore, the *cis*-N_2O_2 configuration seems more probable for the copper binding site in the galactose oxidase.

In recent few years, interesting ENDOR studies on blue copper proteins have been reported.[6,8,9,45] Though complexes having such a type I copper binding site have not been studied in the present work, it seems interesting to compare their data with the present results. It has been shown in the studies that the blue copper proteins, including bean and poplar leaf plastocyanin, azurin, stellacyanin, and fungal laccase, show hf couplings due to two nonequivalent nitrogens having largely different coupling constants (32–49 and 16–24 MHz).[9] By an X-ray analysis,[46] the nitrogens in the poplar plastocyanin and azurin have been assigned to imidazole nitrogens. When compared with the data collected in this work, most of their data are out of the range for the aromatic aza nitrogens in ordinary square-planar copper(II) complexes: one of the two nonequivalent nitrogens shows an extensively smaller coupling and the other shows, in plastocyanin, a larger coupling.

Roberts et al. explained[9] the ^{14}N coupling constants for the blue copper proteins on the basis of the X-ray structure analysis[46] and single-crystal ESR data[47] for poplar plastocyanin. According to the X-ray and single-crystal ESR analyses, the copper ion is coordinated by two imidazole nitrogens (His-37 and His-87, Cu–N = 2.04 and 2.10 Å) and two sulfurs (Cys-84, Cu–S = 2.13 Å; Met-92, Cu–S = 2.90 Å). In the first coordination sphere, N(His-37), N(His-87) and S (Cys-84) are near the unpaired electron orbital plane. N(His-37) and S(Cys-84) are nearly trans to each other, and N(His-87) is nearly cis to N(His-37) and S(Cys-84) but it is below the orbital plane by about 12–20°. On the other hand, S(Met-92) lies nearly normal to the orbital plane with a much larger Cu–S bond length than those of the other donor atoms. Roberts et al. considered that N(His-37) has larger overlap with the unpaired electron d orbital than N(His-87) and assigned the larger coupling constant to N(His-37) and the smaller one to N(His-87). However, in view of the results in this work, an alternative assignment may be possible.

According to the present observation, hf coupling constants of donor atoms are appreciably affected by hybridization of the copper unpaired electron orbital. The hybridization occurs so that a stronger crystalline field from a donor atom leads to less electronic orbital population on the metal in the donor atom direction. In the case of plastocyanin, N(His-37) and S(Cys-84) at the trans positions give the strongest crystalline field to the copper d orbitals, while the crystalline field in the N(His-87)–Cu direction would be much weaker because of the absence of a donor atom at the trans position of N(His-87) and a slightly longer Cu–N bond length than N(His-37)–Cu. Therefore, orbital mixing occurs so that the spread of the unpaired electron orbital becomes small along the N(His-37)–Cu–S(Cys-84) bond direction and expands along the N(His-87)–Cu direction, and this is made by mixing with the 4s orbital. Such unpaired spin distribution on the copper ion may result in larger overlap with N(His-87) than with N(His-37), giving a large ^{14}N(His-87) hf coupling constant and a small ^{14}N(His-37) constant. Absence of a donor atom at the trans position of N(His-87) and strong coordination of N(His-37) and S(Cys-84) may cause a larger mixing effect than in the ordinary *cis*-N_2O_2 donor set seen above and result in a largely different pair of ^{14}N hf couplings. This estimation contradicts to the assignment of Roberts et al., but a preliminary examination made by the use of a MO calculation for a model copper complex supports the estimation.[48]

In the present paper, N_3O type complexes are not treated. ^{14}N ENDOR of this type of complexes is more complex, because of the presence of nonequivalent nitrogens, but for considering structural problems of copper binding sites in type II copper complexes, nitrogen hf interactions in N_3O or N_3X type complexes (X is a donor atom other than N and O) may be more useful.

As shown above, the magnitude of hf couplings of donor nitrogens studied by ENDOR seems very useful for structural investigations if they are used in conjunction with ESR and other spectroscopies.

Registry No. [Cu(dmg)$_2$], 14221-10-4; [Cu(pc)], 147-14-8; [Cu(biu)$_2$]$^{2-}$, 61771-68-4; [Cu(oep)], 14409-63-3; [Cu(tpp)], 14172-91-9; [Cu(amben)], 36527-52-3; [Cu(im$^-$)$_2$], 29503-37-5; [Cu(im)$_4$]$^{2+}$, 47105-83-9; [Cu(im)$_2$(im$^-$)]NO$_3$, 28207-28-5; [Cu(aema)], 22462-62-0; [Cu(im)$_6$]Cl$_2$, 71926-91-5; [Cu(bslal)(H$_2$O)], 101376-94-7; [Cu(slgl)(H$_2$O)], 36748-34-2; [Cu(slal)(H$_2$O)], 15392-76-4; [Cu(nslal)(H$_2$O)], 33339-41-2; [Cu(pyvbl)(H$_2$O)], 66863-18-1; [Cu(pyval)(H$_2$O)], 14284-60-7; [Cu(acen)], 36885-37-7; [Cu(salen)], 14167-15-8; [Cu(salph)], 42490-12-0; [Cu(facen)], 40820-17-5; [Cu(saltn)], 21051-65-0; [Cu(pic)$_2$], 14050-01-2; [Cu(salap)], 14039-58-8; [Cu(sal)$_2$], 14710-63-5; [Cu(esal)$_2$], 14096-19-6; [Cu(npsal)$_2$], 14077-15-7; [Cu(ipsal)$_2$], 14077-14-6; [Cu(nbsal)$_2$], 13986-33-9; [Cu(pymth)$_2$], 13873-22-8; [Cu(ibsal)$_2$], 21051-59-2; [Cu(sbsal)$_2$], 16592-91-9; [Cu(chsal)$_2$], 17084-40-1; [Cu(meqn)$_2$], 14522-43-1; [Cu(qn)$_2$], 10380-28-6; [Cu(tbsal)$_2$], 13986-34-0; [Cu(salox)$_2$], 14363-26-9; [Cu(NH$_3$)$_4$]$^{2+}$, 44001-04-9; [Cu(tn)$_2$]SO$_4$, 49730-81-6; [Cu(eten)$_2$](ClO$_4$)$_2$, 52646-62-5; [Cu(pn)$_2$]SO$_4$, 49730-80-5; [Cu(en)$_2$]SO$_4$, 14099-38-8; [Cu(meen)$_2$]SO$_4$, 52269-00-8; [Cu(glglgl)]$^+$, 21470-85-9; H$_2$[Cu(pdta)], 101376-95-8; H$_2$[Cu(edta)], 54453-03-1; [Cu(en)(H$_2$O)$_2$]SO$_4$, 15293-35-3; [Cu(gly)$_2$], 13479-54-4; [Cu(ala)$_2$], 14263-10-6; [Cu(pro)$_2$], 30955-20-5; [Cu(ser)$_2$], 14221-45-5; [Cu(val)$_2$], 14267-13-1; [Cu(βala)$_2$], 13842-97-2; [Cu(thr)$_2$], 15491-47-1.

(42) Van Camp, H. L.; Sands, R. H.; Fee, J. A. *Biochim. Biophys. Acta* **1982**, *704*, 75.
(43) Tainer, J. A.; Getzoff, E. D.; Richardson, J. S.; Richardson, D. C. *Nature (London)* **1983**, *306*, 284.
(44) (a) Bereman, R. D.; Kosman, D. J. *J. Am. Chem. Soc.* **1977**, *99*, 7322. (b) Kosman, D. J.; Peisach, J.; Mims, W. B. *Biochemistry* **1980**, *19*, 1304. (c) Spiro, T. G. *Copper Proteins*; Wiley: New York, 1981.
(45) (a) Rist, G. H.; Hyde, J. S.; Vanngard, T. *Proc. Natl. Acad. Sci. U.S.A.* **1970**, *67*, 79. (b) Roberts, J. E.; Brown, T. G.; Hoffman, B. M.; Peisach, J. *J. Am. Chem. Soc.* **1980**, *102*, 825.
(46) Colman, P. M.; Freeman, H. C.; Guss, J. M.; Murata, M.; Norris, V. A.; Ramshaw, J. A. M.; Venkatappa, M. P. *Nature (London)* **1978**, *272*, 319. (b) Adam, E. T.; Stenkamp, R. E.; Sieker, L. C.; Jensen, L. H. *J. Mol. Biol.* **1978**, *123*, 35.
(47) Penfield, K. W.; Gay, R. R.; Himmelwright, R. S.; Eickman, N. C.; Norris, V. A.; Freeman, H. C.; Solomon, E. I. *J. Am. Chem. Soc.* **1981**, *103*, 4382.

(48) Details will be published elsewhere.